



SINGLE PHASE GRID CONNECTED FUEL CELL SYSTEM BASED ON BOOST INVERTER

M. Bharati¹ and Ch.Venkata Rajesh²

¹Assistant professor , Dept.of Electrical and Electronics Engineering ,
Sree Venkateswara College of Engineering (JNTUA), Nellore District, A.P.

²Assistant professor , Dept. of Mechanical engineering ,
Sree Venkateswara College of Engineering (JNTUA), Nellore District, A.P.

ABSTRACT

The boost-inverter topology is used as a building block for a single-phase grid-connected fuel cell (FC) system offering low cost and compactness. In addition, the proposed system incorporates battery-based energy storage and a dc-dc bidirectional converter to support the slow dynamics of the FC. The single-phase boost inverter is voltage-mode controlled and the dc-dc bidirectional converter is current-mode controlled. The low-frequency current ripple is supplied by the battery which minimizes the effects of such ripple being drawn directly from the FC itself. Design guidelines, simulation, and experimental results taken from a laboratory prototype are presented to confirm the performance of the proposed system.

KEYWORDS: compactness, ripple, simulation, topology.

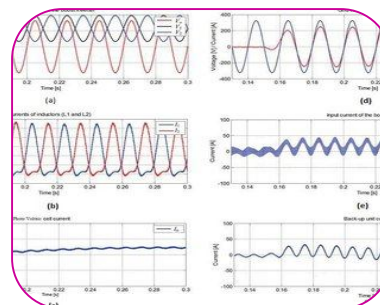
1.0 INTRODUCTON

Alternative energy generation systems based on solar photo voltaic and fuel cells (FCs) need to be conditioned for both dc and ac loads. The overall system includes power electronics energy conversion technologies and may include energy storage based on the target application.

A two-stage FC power conditioning system to deliver ac power has been commonly considered and studied in numerous technical papers. The two-stage FC power conditioning system encounters drawbacks such as being bulky, costly, and relatively inefficient due to its Cascaded power conversion stages. To alleviate these drawbacks, a topology that is suitable for ac loads and is powered from dc sources able to boost and invert the voltage at the same time has been proposed it. The double loop control scheme of this topology has also been proposed for better performance even during transient conditions. [orpalladium](#)) for higher efficiency. [Carbon paper](#) separates them from the electrolyte. The electrolyte could be a ceramic or a membrane.

In our proposed project, we consider PEMFC because it is the most reliable and produce a less compact structure. The number of cells used in this design are less as they have a simple structure and can result in higher efficiency which there by increases the continuity of supply. In these days PEMFC is used exclusively to retain better and loss less power.

1.27 Power Conditioning Systems (PCS): A Power Conditioning System (PCS) with energy storage capability can be considered a viable solution for improving the quality and the reliability of the electric energy supply. Several tasks can be performed at the same time, such as reactive power compensation, current harmonic reduction, and



smoothing of pulsating loads. Moreover, the PCS can operate as Uninterruptible Power Supply (UPS) during short time interruptions of the grid supply. The proposed PCS is a flexible structure that can be coupled to several energy storage devices like battery, flywheel, super capacitor, Superconductive magnetic energy storage (SMES). These new storage devices allow additional tasks to be performed using the same hardware structure required for the UPS operation. The additional tasks consist of reactive power compensation, current harmonic reduction, load unbalance compensation, and smoothing of pulsating loads. In this way, the UPS behaves as a Power Conditioning System (PCS) when the grid supply is present, improving significantly the power quality in the grid section next to the Point of Common Coupling (PCC).

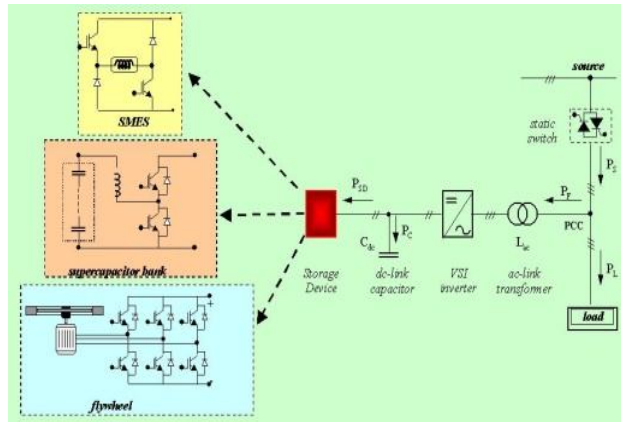


Fig 1.2: Schematic diagram of PCS

Transmission capacities are known as super, or mega grids. The promised benefits include enabling the renewable energy industry to sell electricity to distant markets, the ability to increase usage of intermittent energy sources by balancing them across vast geological regions, and the removal of congestion that prevents electricity markets from flourishing. Local opposition to siting new lines and the significant cost of these projects are major obstacles to super grids.

1.4 Block Diagram of Boost Inverter:

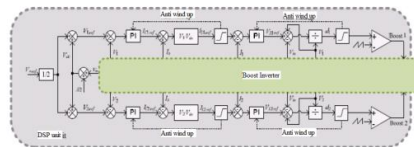


Fig 3.4 Block diagram of the boost controlled inverter

1.3 AC Gain Characteristics of Boost Inverter

For the condition, switch S_1 is open and S_2 is closed, as shown in figure, the inductor current iL_1 flows through capacitor C_1 and load. The current iL_1 decreases while capacitor C_1 is recharged.

Since output voltage in equation is twice the sinusoidal component of converter A, the peak output voltage equals to

$$V_{opeak}=2V_m=2V_1-2V_{dc}$$

Because a boost converter cannot produce a output voltage lower than the input voltage, the dc component must satisfy

$$V_{dc} \geq (V_m + V_{in})$$

This implies there are many possible values of V_{dc} . However, equal term produces the least stress on the devices. From the above two equations we get

$$V_{o(\text{peak})} = (2V_{in}/1-K) - (V_{o(\text{peak})} + 2V_{in})$$

Thus $V_{o(\text{peak})}$ becomes V_{in} at K equal to 0.5. The ac and dc gain characteristics of the boost inverter are shown in figure. The inductor current I_L that depends on the load resistance R and duty cycle K , can be found from,

$$G_{ac} = V_{o(\text{peak})}/V_{in} = K/1-K$$

The voltage stress of the boost inverter depends on the ac gain G_{ac} , the peak output voltage V_m and the load current I_L .

$$I_L = (K/1-K)(V_{in}/1-K)$$

2.0 DC GAIN CHARACTERISTICS OF BOOST INVERTER:

The condition, switch S_1 is closed and S_2 is open as shown in figure, the inductor current i_{L1} raises quite linearly, diode D_2 is reversed biased, capacitor C_1 supplies energy to the load, and Voltage V_1 decreases. The average output voltage of converter A, which operates under the boost mode, is given by

$$V_1 = (V_{in}/1-K)$$

The average output voltage of converter B, which operates under the buck mode, is given by,

$$V_2 = (V_{in}/K)$$

$$V_0 = V_1 - V_2 = (V_{in}/1-K) - (V_{in}/K)$$

the boost inverter output voltage and power ratings are selected, inductances L_1 and L_2 are designed from output switching frequency is selected from the converter ratings and switch type. Let we want to design the inverter for resistive load of $P_o = 500\text{Watt}$, switching frequency = 3 KHz, $V_{in} = 150\text{V}$ and $V_o = 220\text{Vrms}$.

The selection of the value of inductor and capacitor is based on the minimum ripples in output current and voltage. Now for output voltage $V_o = 311(\sin 314t)$, first the DC component of the capacitor voltage is calculated from the equations

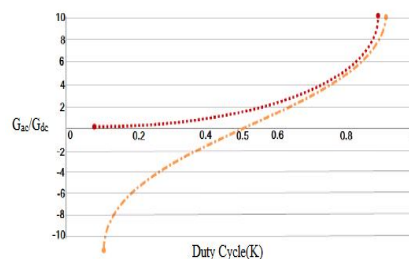


Fig 3.6 Gain Characteristics of Boost Inverter

2.1. IGBT Mechanism:

IGBT is a three-terminal power semiconductor device, noted for high efficiency and fast switching. It switches electric power in many modern appliances: electric cars, trains, variable speed refrigerators, air-conditioners and even stereo systems with switching amplifiers. Since it is designed to rapidly turn on and off, amplifiers that use it often synthesize complex waveforms.

The IGBT combines the simple gate-drive characteristics of the MOSFETs with the high-current and low-saturation-voltage capability of bipolar transistors by combining an isolated gate FET for the control input, and a bipolar power transistor as a switch, in a single device.

The IGBT is used in medium- to high-power applications such as switched-mode power supply, traction motor control and induction heating. Large IGBT modules typically consist of many devices in parallel and can have very high current handling capabilities in the order of hundreds of amperes with blocking voltages of 6000 V, equating to hundreds of kilowatts.

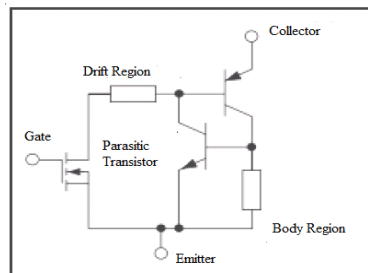


Fig 2.1. Equivalent circuit of IGBT

The IGBT is a fairly recent invention. The first-generation devices of the 1980s and early 1990s were relatively slow in switching, and prone to failure through such modes as latch up (in which the device won't turn off as long as current is flowing) and secondary breakdown (in which a localized hotspot in the device goes into thermal runaway and burns the device out at high currents).

The extremely high pulse ratings of second- and third generation devices also make them useful for generating large power pulses in areas like particle and plasma physics, where they are starting to supersede older devices like thyratrons and triggered spark gaps.

Their high pulse ratings, and low prices on the surplus market, also make them attractive to the high-voltage hobbyist for controlling large amounts of power to drive devices such as solid-state Tesla coils and coil guns. Availability of affordable, reliable IGBTs is an important enabler for electric vehicles.

2.2. PROPOSED FC ENERGY SYSTEM

2.2.1 Description of FC system

The block diagram of the proposed grid-connected FC system is shown in Fig. 4.1(b). Fig. 4.1(b) also shows the power flows between each part. This system consists of two power converters: the boost inverter and the bidirectional backup unit, as shown in Figs. 4.1(b). Fig. 4.1(a) shows the laboratory setup of the proposed FC system. The boost inverter is supplied by the FC and the backup unit, which are both connected to the same unregulated dc bus, while the output side is connected to the load and grid through an inductor. The system incorporates a current-mode controlled bidirectional converter with battery energy storage to support the FC power generation and a voltage-controlled boost inverter.

The FC system should dynamically adjust to varying input voltage while maintaining constant power operation. Voltage and current limits, which should be provided by the manufacturers of the FC stack, need to be imposed at the input of the converter to protect the FC from damage due to excessive loading and transients. Moreover, the power has to be ramped up and down so that the FC can react appropriately,

avoiding transients and extending its lifetime. The converter also has to meet the maximum ripple current requirements of the FC.

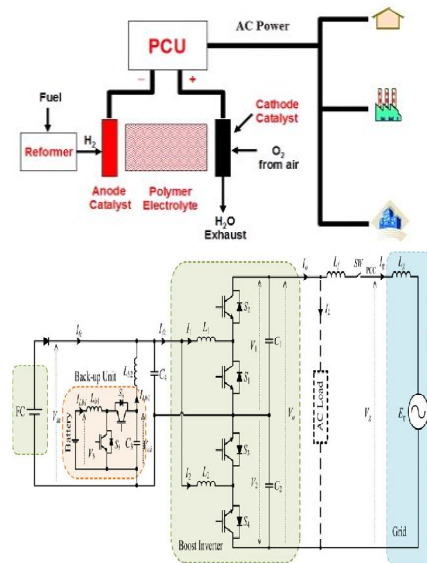


Fig. 2.2.1(b) General structure of the proposed grid-connected FC system

In the grid-connected mode, the system is also providing active (P) and reactive (Q) power control. A key concept of the PQ control in the inductive coupled voltage sources is the use of a grid compatible frequency and voltage droops. Therefore, the active and reactive powers are controlled by the small variations of the voltage phase and magnitude. The control of the inverter requires a fast signal conditioning for single-phase systems. In the proposed system, the second-order generalized integrator (SOGI) algorithm has been employed.

2.3 Boost Inverter:

The boost inverter consists of two bidirectional boost converters and their outputs are connected in series, as shown in Fig. 3. Each boost converter generates a dc bias with deliberate ac output voltage (a dc-biased sinusoidal waveform as an output), so that each converter generates a uni polar voltage greater than the FC voltage with a variable duty cycle. Each converter output and the combined outputs are described by

$$\begin{aligned}
 V_1 &= V_{dc} + 0.5 \cdot A_1 \cdot \sin \theta \\
 V_2 &= V_{dc} + 0.5 \cdot A_2 \cdot \sin (\theta - \pi) \\
 V_0 &= V_1 - V_2 = A_0 \cdot \sin \theta, \\
 \text{When } A_0 &= A_1 = A_2 \quad V_{dc} > V_{in} + 0.5 A_0
 \end{aligned}$$

Where V_{dc} is the dc offset voltage of each boost converter and have to be greater than $0.5 A_0 + V_{in}$. From (3), it can be observed that the output voltage V_0 contains only the ac component.

This concept has been discussed in numerous papers. The boost inverter employs voltage mode control. In this paper, a double-loop control scheme is chosen for the boost-inverter control being the most appropriate method to control the individual boost converters covering the wide range of operating points. This control method is based on the averaged continuous-time model of the boost topology and has several advantages with special conditions that may not be provided by the sliding mode control, such as nonlinear loads, abrupt load variations, and transient short-circuit situations. Using this control method, the inverter

maintains a stable operating condition by means of limiting the inductor current. Because of this ability to keep the system under control even in these situations, the inverter achieves a very reliable operation.

The reference voltage of the boost inverter is provided from the PQ control algorithm being able to control the active and reactive power. The voltages across C_1 and C_2 are controlled to track the voltage references using proportional-resonant (PR) controllers. Compared with the conventional proportional integral (PI) controller, the PR controller has the ability to minimize the drawbacks of the PI one such as lack of tracking a sinusoidal reference with zero steady-state error and poor disturbance rejection capability.

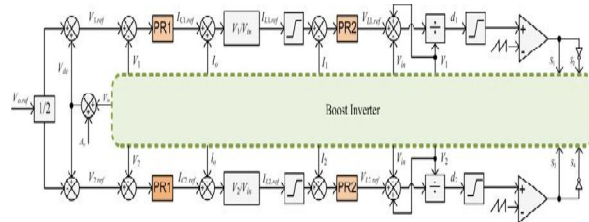


Fig. 2.3. Boost-inverter control block diagram.

The currents through L_1 and L_2 are controlled by PR controllers to achieve a stable operation under special conditions such as nonlinear loads and transients. The control block diagram for the boost inverter is shown in Fig.4.2. The output voltage reference is divided to generate the two individual output voltage references of the two boost converters with the dc bias, V_{dc} . The dc bias can be obtained by adding the input voltage V_{in} to the half of the peak output amplitude. V_{dc} is also used to minimize the output voltages of the converters and the switching losses in the variable input voltage condition. The output voltage reference is determined by

$$V_{0ref}=(V_{pp}+dV_{pp})\cdot\sin(W_{0t}+\varphi), \quad A_0=V_{pp}+dV_{pp} \text{ and } \theta=W_{0t}+\varphi$$

where V_{pp} is the peak value of the typical grid voltage, dV_{pp} is a small variation of the output voltage reference affecting to the reactive power, W_0 is the grid fundamental angular frequency, and φ is the phase difference between V_o and V_g relating with the active power. Then, $V_{1.ref}$ and $V_{2.ref}$ are calculated by (1) and (2).

2.4. Backup Energy Storage Unit:

The functions of the backup energy storage unit are divided into two parts. First, the backup unit is designed to support the slow dynamics of the FC. Second, in order to protect the FC system, the backup unit provides low-frequency ac current that is required from the boost inverter operation.

The low-frequency current ripple supplied by the batteries has an impact on their lifetime, but between the most expensive FC components and the relatively inexpensive battery components, the latter is preferable to be stressed by such low-frequency current ripple.

The backup unit comprises of a current-mode controlled bidirectional converter and a battery as the energy storage unit. For instance, when a 1-kW load is connected from a no-load condition, the backup unit immediately provides the 1-kW power from the battery to the load, as shown in Table 4.3. On the other hand, when the load is disconnected suddenly, the surplus power from the FC could be recovered and stored into the battery to increase the overall efficiency of the energy system.

The backup unit controller is designed to control the output current of the backup unit in Fig. The reference of i_{Lb1} is determined by I_{dc} through a high-pass filter and the demanded current I_{demand} that is related to the load change. The ac component of the current reference deals with eliminating the ac ripple current into the FC power module while the dc component deals with the slow dynamics of the FC.

Table 2.3: Backup unit sequence under loads of operation.

P3 Increase (P1+P2=P3)	P3Decrease (P1=P2+P3)	Normal (P1=P3)
Discharge	-	-
Charge	Charge	Charge
Normal	Normal	Normal

2.4 Control of a grid connected boost inverter

The equivalent circuit of the grid-connected FC system consisting of two ac sources (V_g and V_o), an ac inductor L_f between the two ac sources, and the load. The boost inverter output voltage (including the FC and backup unit) is indicated as V_o and V_g is the grid voltage. The active and reactive powers at the point of common coupling (PCC) are expressed

$$P=(V_g \cdot V_o \cdot \sin\alpha)/W_0 \cdot L_f$$

$$Q=(V_g^2/w_0 \cdot L_f)-\{(V_g \cdot V_o)/(W_0 \cdot L_f)\}$$

where L_f is the filter inductance between the grid and the boost inverter. The phase shift α and voltage difference $V_g - V_o$ between V_o and V_g affect the active and the reactive powers, respectively. Therefore, to control the power flows between the boost inverter and the grid, the FC system must be able to vary its output voltage V_o in amplitude and phase with respect to the grid voltage V_g .

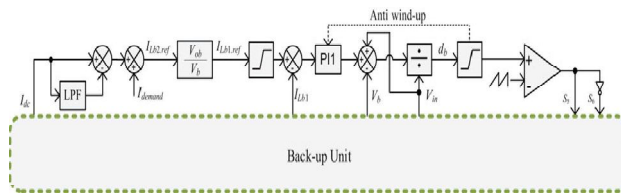


Fig. 2.4. Backup unit control block diagram

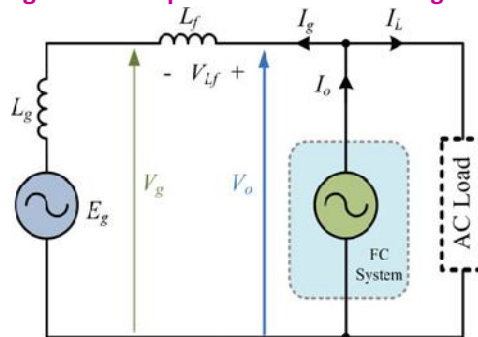


Fig. 2.4. Equivalent circuit of the grid-connected FC system

According to these vector diagrams, power flow, active power and reactive powers should be controlled by the phase angle δ and the inverter voltage amplitude, V_o . For instance, when the reactive power reference is zero, Fig. 4.4.4(a) shows active power controlling with small variations of δ and dV_{pp} . If active and reactive powers need to be controlled simultaneously, Fig. 4.4.4(b) is the approach to control them.

Fig. 2.4. Illustrates that only dV_{pp} is controlled for reactive power while the active power is zero by the magnitude of V_o equals V_g . Fig. 4.4.4 illustrates that the system is sensitive to small changes of the phase δ and the magnitude dV_{pp} .

Therefore, the grid connected FC system as parallel operation of voltage source inverters requires a precise control. Grid-compatible frequency and voltage droop were introduced to control active and reactive powers in this paper. The droop control for the boost inverter requires the fast acquisition of P and Q. The measurement of P and Q at the PCC is obtained based on the following expressions:

$$P_{meas} = 0.5(V_{g\alpha} \cdot i_{g\alpha} + V_{g\beta} \cdot i_{g\beta})$$

$$Q_{meas} = 0.5(V_{g\beta} \cdot i_{g\alpha} - V_{g\alpha} \cdot i_{g\beta})$$

where $v_{g\alpha}$ and $v_{g\beta}$ are the instantaneous orthogonal voltages at PCC, and $i_{g\alpha}$ and $i_{g\beta}$ are the instantaneous orthogonal currents at PCC.

The orthogonal voltage and current are obtained using a SOGI-based algorithm which provides a fast signal conditioning for single-phase systems. Fig. 2.4. Illustrates the PQ control algorithm with the phase locked loop and the orthogonal system generator. δ and dV_{pp} are determined by PI regulators to track the active and reactive power references. The inverter voltage reference is generated to control the active and reactive powers using the droop control method, as shown in Fig. 4.4.3

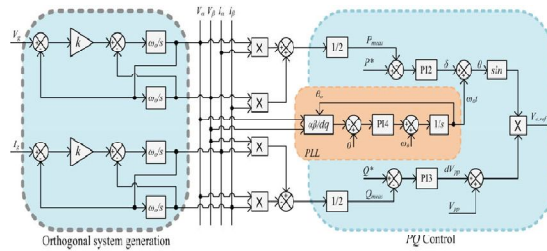


Fig. 2.4. Boost-inverter output voltage reference generation block diagram with the PQ control algorithm.

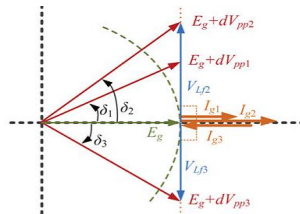


Fig.2.4. Vector diagram when reactive power reference is zero

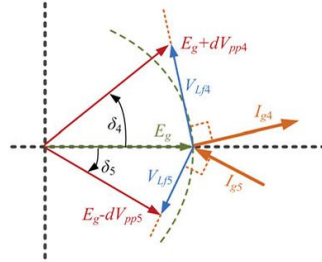


Fig.2.4.Vector diagram when active and reactive powers are controlled simultaneously.

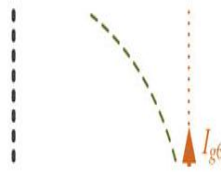


Fig.4.4.6 Vector diagram when active power reference is zero

3.0 DESIGN GUIDELINES:

The power components of the proposed system were designed with the parameters given in Table II.

FC output voltage	36-69V(72-cell FC)
AC output voltage	220V RMS,single phase,50HZ
AC grid voltage	220V,50HZ
Switching Frequency	20KHZ
Output power	1KW
V_{in}	42V(min)
Ra(resistance of L1 and L2)	$\approx 10m\Omega$
$V_1(t)$	353(max)
$V_2(t)$	42V(min)
Δt_1 (maximum on time)	42.5microseconds(max at 20KHZ)
Δi_{Lmax}	5% of I_{Lmax}
$R_{1(load)}$	48.4 Ω at 1KW
ΔV_c	5% of V_{1max}
Vb(battery voltage)	22V(min)-27.3V(max)

Table 3.0. Specifications of FC system

The current of the inductors (i_{L1} , i_{L2}) consists of fundamental and switching frequency components. To calculate the inductance of L_1 and L_2 , the following equations are used where $i_L(max)$ is maximum inductor current and Δi_L is highfrequency ripple current of the inductor caused by switching.

$$i_L(max) = (V_{in} - \sqrt{V_{in}^2 + 4R_a(V_1(t)) \cdot (V_2(t) - V_1(t)) / R_1}) / 2R_a$$

$$\Delta i_L(t) = (V_{in} - R_a \cdot i_L(t)) \cdot \Delta t_1 / L$$

The maximum inductor current ripple Δi_{Lmax} is chosen to be equal to 5% of the maximum inductor current, as calculated from (10) when the V_1 is maximum and V_2 is minimum. From above equations, the minimum inductance is calculated as 650 and 700 μH which are the chosen values for L_1 and L_2 .

$$\Delta V_c = (V_1(t) - V_2(t)) \cdot \Delta t_1 / C \cdot R_1$$

A 15- μ F designed capacitor value has been obtained using and a 20- μ F 800-V rated metalized polypropylene film capacitor has been used as C_1 and C_2 for the experimental setup, as shown. The same value of 20 μ F has been used for the backup unit capacitors C_3 and C_4 . During transient conditions, the backup unit should provide all the power required by the load. In this case, the maximum inductor current of the boost inverter should appear in the inductor L_{b2} . Therefore, maximum inductance of L_{b2} can be calculated by above eq. and $\Delta i_L(t)_{max}$ need to be larger than the maximum inductor current of the boost inverter in order to track the maximum slope of the current. The maximum inductance is obtained as 366 μ H and the values of L_{b1} and L_{b2} are chosen to be 150 μ H

Power stack	SEMISTACK-IGBT
Controller	DPTMS320F28335
Voltage transducers	LEM LV25-P
Current transducers	LEM HAL50s
Energy storage	Two 12V-24Ah lead acid batteries
$L_1=L_2$	700microH
$L_{b1}=L_{b2}$	150microH
L_f	5microH
$C_1=C_2=C_3=C_4$	20microF
PR_1	$K_p:0.1, K_i:10$
PR_2	$K_p:1, K_i:1000$
P_{11}	$K_p:0.1, K_i:100$
P_{12}	$K_p:1e^{-6}, K_i:1e^{-3}$

Table: 4.7.2 Specifications for the FC system

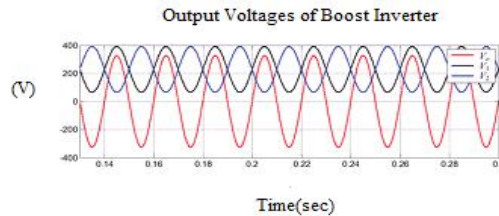


Fig 3.1 output voltages of the boost inverter

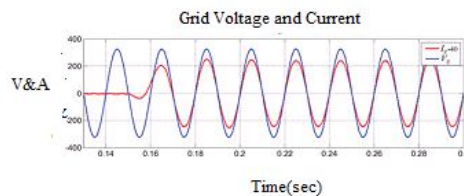


Fig 3.2 Grid voltages and current

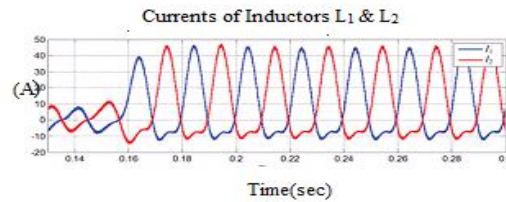


Fig 3.3 Currents of inductors (L1 and L2)

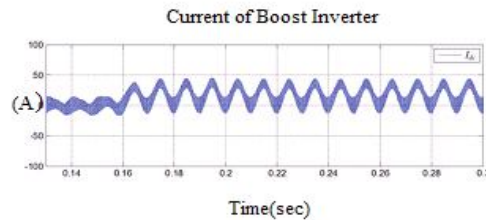


Fig 3.4 Input current of the boost inverter

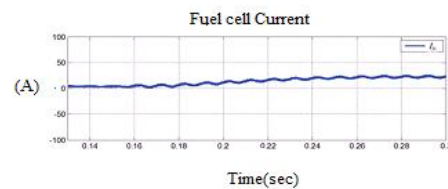


Fig 3.5 Fuel current

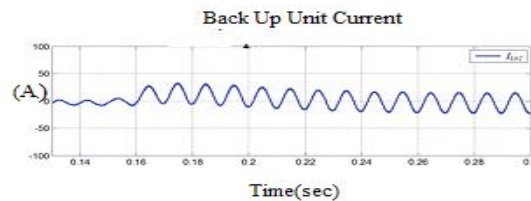


Fig 3.6. Back up unit current

The capacity of the battery should be designed to recover the slow dynamics (maximum current slew rate is 4 A/s [12]) and start up time (30 s at room temperature [5]) of the FC. Two generic 12-V lead-acid batteries are introduced for energy storage to deal with the need to provide fast dynamics and a relatively low-cost solution. The FC startup time should be considered as worst case scenario to calculate the battery capacity.

The minimum and maximum voltages of the battery are shown in Table II. The battery consists of six cells and recommended float voltage for the batteries at 25 °C is 2.26 V/cell and the capacity choice guideline is provided in the battery's manual [25]. To find the minimum voltage per cells, the minimum voltage of the battery is divided by the number of cells ($22/12 = 1.833$ V/cell).

The load Watts per cell is obtained as the rated power divided by the number of cells ($1000/12 = 83.33$ W/cell). The value of Watts per cell per Ah can be found at 4.13 in the provided Watts/Ah/Cell table [25]. The minimum battery capacity is obtained as the load Watts per cell divided by the value from the Watts/Ah/Cell table ($83.33/4.13 = 20$ Ah). Therefore, a 24-Ah battery is selected for the system.

4.0 SIMULATION CIRCUITS AND RESULTS:

4.1 Simulation Circuits

The proposed FC system (see Fig. 3) has been analyzed, designed, simulated, and tested experimentally to validate its overall performance. The simulations have been done using Simulink/MATLAB and PLECS block set to validate the analytical results. The ac output voltage of the system was chosen to be equal to 220 V, while the dc input voltage varied between 43 and 69 V. The obtained experimental efficiency for the proposed system is about 93% at peak point and 83% at rated output power. Consequently, the proposed FC system achieves an increased total efficiency when compared with a conventional two-stage FC system.

The proposed single-phase grid-connected FC system has been developed as a laboratory prototype (see Fig. 4). In this paper, a dc power supply is used to provide dc output between 43 and 69V, same voltage range as a 72-cell PEMFC. The power electronic stack consists of three insulated gate bipolar transistor (IGBT) modules that are used to build the boost inverter for two modules and backup unit for one module. The DSP controller unit has been used for a number of reasons such as low cost.

Simulation block diagram

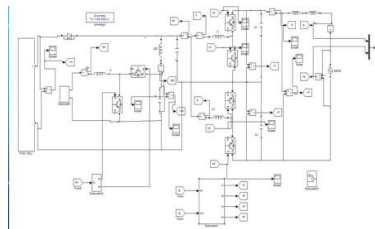


Fig 5.1(a) Simulation circuit of the proposed FC system

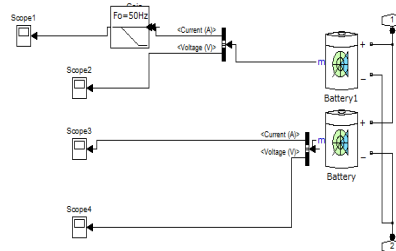


Fig 5.1(b) Simulation circuit of Battery backup unit

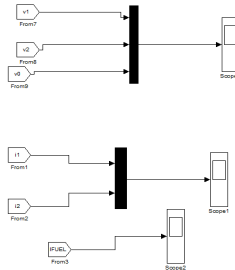


Fig 5.1(c) simulation circuit of FC system

5.2 Simulation Outputs

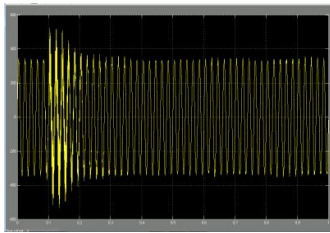


Fig 5.2(b) Output voltage of the boost inverter

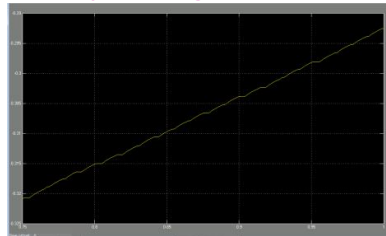


Fig 5.2(c) Fuel cell current

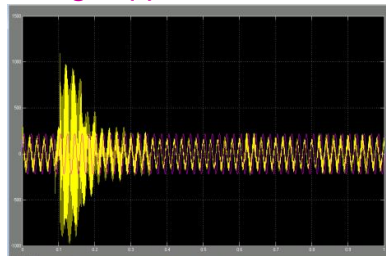


Fig 5.2(d) Grid output voltage and current

The simulation results show the operations of the boost inverter and the backup unit. In particular, Fig.5.2 (b) illustrates the output voltages of the boost inverter (V_1 , V_2 , and V_o) and Fig. 5.2(d) shows the grid voltage and grid current at the PCC. The input currents of each boost converter flowing through the inductors L_1 and L_2 are shown in Fig. 5.2(a).

Fig. 5.2(c) illustrates the waveforms of the inverter input current I_{dc} , the FC output current I_{fc} , and the output current I_{Lb2} of the backup unit, respectively. When full-load is required from the no-load operating point, the entire power is provided by the backup unit to the load. Then, the power drawn from the battery starts decreasing moderately allowing gentle step-up to deliver power which should increase up to meet the demanded load power.

Experimental results for the grid connection of the FC system are presented in Fig. 5.2(d) illustrates the current through the inductor L_f and the voltages of grid and inverter output (V_g and V_o). The difference between the two voltages is not visible due to the small amount of the phase angle being under

0.01[rad].The fast Fourier transform (FFT) of the grid current I_g with the total harmonic distortion (THD) being approximately 4% which shows the active and reactive power control performance.

6.0 CONCLUSION:

A single-phase single power stage grid-connected FC system based on the boost-inverter topology with a backup battery based energy storage unit is proposed in this project. The simulation results and selected laboratory tests verify the operation characteristics of the proposed FC system. In summary, the proposed FC system has a number of attractive features, such as single power conversion stage with high efficiency, simplified topology, low cost, and able to operate in stand-alone as well as in grid-connected mode. Moreover, in the grid-connected mode, the single-phase FC system is able to control the active and reactive powers by a PQ control algorithm based on SOGI which offers a fast signal conditioning for single-phase systems. However, it should be noted that the voltage-mode control adopted for the boost inverter may result in a distorted grid current (under given THD) if the grid voltage includes a harmonic component.

6.1 Future Scope:

Due to this energy crisis and environmental issues, renewable energy sources have attracted the attention of Researches and Investors. Among all the renewable sources, fuel cells systems are considered as the most promising technology because of its suitability. In the proposed system, the FC system is interfaced with the grid more efficiently. The drawback of this system is, the topology is designed for single phase systems. The future scope for this project is, this can also be extended to three phase systems by using three phase inverters. This topology is also useful in interfacing the FC system with smart grid more efficiently.

7. REFERENCES

- [1] S. B. Kjaer, J. K. Pedersen, and F. Blaabjerg, "A review of single-phase grid-connected inverters for photovoltaic modules," *IEEE Trans. Ind. Appl.*, vol. 41, no. 5, pp. 1292–1306, Sep./Oct. 2005.
- [2] S. B. Kjaer, "Design and control of an inverter for photovoltaic applications," Ph.D. dissertation, Inst. Energy Technol., Aalborg Univ., Aalborg, Denmark, 2005.
- [3] J.-S. Lai, "Power conditioning circuit topologies," *IEEE Ind. Electron. Mag.*, vol. 3, no. 2, pp. 24–34, Jun. 2009.
- [4] M. E. Schenck, J.-S. Lai, and K. Stanton, "Fuel cell and power conditioning system interactions," in *Proc. IEEE Appl. Power Electron. Conf. Expo.*, Mar. 2005, vol. 1, pp. 114–120.
- [5] Horizon Fuel Cell Technologies, H-Series PEMFC System User Guide (2010). [Online]. Available: <http://www.horizonfuelcell.com>
- [6] J. Anzicsek and M. Thompson, "DC-DC boost converter design for Kettering University's GEM fuel cell vehicle," in *Proc. Electr. Insul. Conf. Electr. Manuf. Expo.*, 2005, pp. 307–316.
- [7] X. Yu, M. R. Starke, L. M. Tolbert, and B. Ozpineci, "Fuel cell power conditioning for electric power applications: A summary," *IET Electr. Power Appl.*, vol. 1, pp. 643–656, 2007.
- [8] K. Jin, X. Ruan, M. Yang, and M. Xu, "Power management for fuel-cell power system cold start," *IEEE Trans. Power Electron.*, vol. 24, no. 10, pp. 2391–2395, Oct. 2009.



M. Bharati

Assistant professor , Dept.of Electrical and Electronics Engineering ,
Sree Venkateswara College of Engineering (JNTUA), Nellore District, A.P.